

# Rapid Test Methods for Analyzing Degradable Polyolefins with a Pro-Oxidant System

F. KHABBAZ, A. C. ALBERTSSON

Department of Polymer Technology, Royal Institute of Technology (KTH), S-100 44 Stockholm, Sweden

Received 2 May 2000; accepted 30 May 2000

**ABSTRACT:** Chemiluminescence, size exclusion chromatography, differential scanning calorimetry, thermogravimetry, and Fourier transform infrared spectroscopy were used to assess differences in oxidation rate between two different pro-oxidant systems in degradable low-density polyethylene. The pro-oxidant formulation used consisted of manganese stearate and natural rubber or manganese stearate and a synthetic, styrene-butadiene copolymer rubber. The low-density polyethylene containing the pro-oxidant with natural rubber showed the highest degradation rate. Chemiluminescence and thermogravimetry were found to be the most effective techniques for establishing the differences between different pro-oxidant systems. © 2001 John Wiley & Sons, Inc. *J Appl Polym Sci* 79: 2309–2316, 2001

**Key words:** degradable low-density polyethylene; thermo-oxidation; pro-oxidant; chemiluminescence; thermogravimetry

## INTRODUCTION

In the last two decades, the use of plastic films for greenhouse and mulch applications to achieve maximum production has increased steadily all over the world. The disadvantages of using mulch film are the need for removal after the harvesting season and the cost associated with it. However, leaving used mulch film in the field leads to ecological problems in the outdoor environment, because polyolefins in their pure form are extremely resistant to degradation.<sup>1,2</sup> It has been estimated that polyethylene would degrade less than 0.5% in 100 years, and 1% if exposed to sunlight for 2 years before biodegradation.<sup>2</sup> An excellent way to make polyolefin materials degradable is to blend them with pro-oxidant additives, which can effec-

tively enhance the degradability of these materials.<sup>3,4</sup> In several patents and articles between 1970 and 1991, Griffin<sup>5–8</sup> claimed that degradable polyolefin compositions can be obtained by using transition metal salts with fatty acids, esters, natural oils, unsaturated elastomers, and corn starch.

We have shown in previous studies<sup>9–12</sup> that polyethylene containing a pro-oxidant additive has a greater susceptibility to degradation by ultraviolet radiation and heat. The pro-oxidant produces free radicals that attack the molecular structure of the polyolefins chain, and this leads to auto-oxidation reactions.<sup>13</sup> The auto-oxidation is initiated by the production of radicals because of the breaking of chemical bonds. The scission occurs preferentially in weak links, i.e., in bonds with a lower bond dissociation energy than normal, e.g., unsaturated bonds.

By suitable selection of the pro-oxidant system and conditions, the molecular weight can decrease rapidly to a level that is low enough for the biodegradation process to proceed. The choice of

---

Correspondence to: A. C. Albertsson.

Contract grant sponsor: Swedish Research Council for Engineering Science, TFR; contract grant number: 35000-601 01.

*Journal of Applied Polymer Science*, Vol. 79, 2309–2316 (2001)  
© 2001 John Wiley & Sons, Inc.

the pro-oxidant system is therefore very important in the design of degradable mulch film.

Different techniques have been used to monitor the degradation of polyethylene.<sup>9,12</sup> The aim of this study was to test different techniques to determine the differences among various pro-oxidant systems and their abilities to enhance the degradation of low-density polyethylene (LDPE) during thermo-oxidation. The thermo-oxidation of LDPE containing two different pro-oxidant systems [manganese stearate and styrene-butadiene rubber (SBR)/or natural rubber (NR)] was conducted in an oven in the presence of air at 60 and 100°C for periods of 14 days. The effect of the pro-oxidant system on the thermo-oxidation of LDPE was evaluated by using chemiluminescence (CL), size exclusion chromatography (SEC), differential scanning calorimetry (DSC), thermogravimetry (TGA), and Fourier transform infrared spectroscopy (FTIR).

## EXPERIMENTAL

### Materials

LDPE films with a thicknesses of 37  $\mu\text{m}$  were used in this study. These films were made by a conventional blown-film process using a Betol extruder. The extruder had a screw diameter of 25 mm and a length-to-diameter ratio of 20:1. The LDPE used was made by the ATO Company (France) and had an Melt Flow Index (MFI) of 2 and a density of 0.918 g/mL.

The samples contained 3% (wt %) pro-oxidant additive. The pro-oxidant consisted of either 1% manganese stearate and 2% styrene-butadiene copolymer (SBS), denoted LDPE-SBR, or 1% manganese stearate and 2% natural rubber, denoted LDPE-NR. The manganese stearate content corresponded to 100 ppm of Mn. Samples without additives were used as control samples and denoted LDPE. All samples were kindly provided by Epron Industries Ltd., Lincolnshire, U.K.

### Degradation Procedure

Thermo-oxidation was performed in an oven in the presence of air. Approximately 1-g samples were placed in glass beakers and held at 60 or 100°C for a period of 14 days.

The unaged polyethylene films and films aged at 60 and 100°C were designated as LDPE-unaged,

LDPE-SBR-unaged, LDPE-NR-unaged, LDPE-60°C, LDPE-SBR-60°C, LDPE-NR-60°C, LDPE-100°C, LDPE-SBR-100°C, and LDPE-NR-100°C.

### Methods

#### CL

CL measurements were performed by using a CL instrument from Tohoku Electronic Industrial Co., Japan, equipped with a CLD 100 CL-detector. The measurements were performed under isothermal conditions in a synthetic air atmosphere at 100°C with a gas flow rate of 70 mL/min for a period of 14 days.

#### SEC

A Waters 150CV high temperature SEC was used to study the changes in molecular weight. The instrument was equipped with a refractive index detector and two PLgel mixed bed-B columns (30 cm, 10  $\mu\text{m}$ ). 1,2-Dichlorobenzene with antioxidant (Santonox R) was used as mobile phase at 140°C at a flow rate of 1 mL/min.

#### DSC

DSC was used to measure the changes in crystallinity and melting behavior in the different materials. Melting endotherms were obtained using a Mettler-Toledo 820 DSC at a heating and cooling rate of 10°C/min on samples weighing 5–7 mg. Thermograms for samples were recorded in three consecutive runs: 1. a first heating from 30 to 150°C, followed by 2. cooling from 150 to 30°C, and finally 3. a second heating from 30 to 150°C. The calorimeter was calibrated using an Indium/Zinc sample. The crystallinity of the samples was determined from the ratio of the melting enthalpy for the samples to the melting enthalpy for 100% crystalline polyethylene, assumed to be 293 J/g.<sup>14</sup> The melting temperature was taken at the maximum of the endothermic peak. In each case, the results were based on the analysis of three separate samples.

#### TGA

TGA analysis was performed in a Mettler-Toledo TGA/SDTA 851° system in an oxygen atmosphere at 100°C for a period of 14 days. The gas flow rate was 50 mL/min. About 22 mg of sample was used for each experiment.

#### FTIR

The changes in the carbonyl region during oxidation were determined by using a Perkin-Elmer

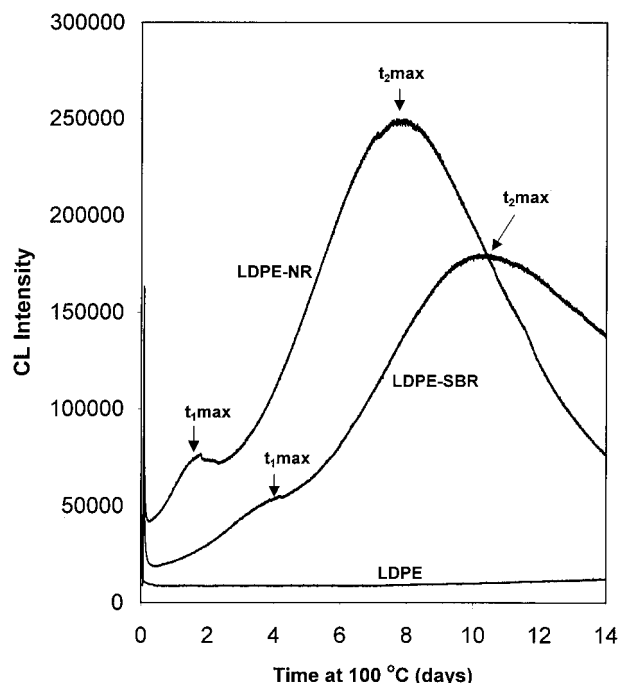


**Figure 1** CL intensity as a function of time for LDPE, LDPE-SBR, and LDPE-NR. The isothermal measurements were made at 100°C over a period of 14 days in an air atmosphere.

2000X FTIR spectrometer equipped with a Golden Gate single reflection ATR unit with a diamond crystal, with an angle of incidence of 40° (P/N 10500 series from Graseby Spectra). The resulting spectrum was an average of 20 scans at 4 cm<sup>-1</sup> resolution.

## RESULTS AND DISCUSSION

The CL technique measures the weak luminescence that is emitted as a result of oxidative re-

actions.<sup>15-18</sup> Figure 1 presents the CL curves for the LDPE, LDPE-SBR, and LDPE-NR at 100°C obtained over a period of 14 days. The oxidation induction time is almost the same for the LDPE-SBR and LDPE-NR samples. As shown in Figure 1, oxidation takes place in two stages in the LDPE-SBR and LDPE-NR samples. The first stage corresponds to the oxidation of the NR and SBR parts of the pro-oxidant in the LDPE-SBR and LDPE-NR samples. The NR parts in the LDPE-NR samples oxidize faster ( $t_{1,max}$  about 2 days) than the SBR parts in the LDPE-SBR samples ( $t_{1,max}$  about 4 days). The rate of oxidation is faster for the LDPE-NR than for the LDPE-SBR samples even in the second stage. The degradation ends over a shorter period ( $t_{2,max}$  about 8 days) for the LDPE-NR samples than for the LDPE-SBR samples ( $t_{2,max}$  about 10 days). The maximum intensity of the CL signals is also higher for the LDPE-NR samples than for the LDPE-SBR samples. This is because the final damaging effect of the pro-oxidant in LDPE-NR is higher than that of the pro-oxidant in LDPE-SBR samples. LDPE samples did not show any significant CL intensity during the test period.

It has been shown that CL emitted during the oxidation of polymers correlates well with the oxygen uptake,<sup>16</sup> which indicates that the intensity is proportional to the rate of oxidation. The most significant parameter for pro-oxidant efficiency is the rate of oxidation of the rubber phase, because there is a large amount of unsaturation in this phase.<sup>19</sup> During the initial phase of degradation, the rubber phase in the pro-oxidant additive is converted to hydroperoxides which decompose when heated. Transition metal salts catalyze the decomposition of hydroperoxides, leading to the generation of free radicals which initiate the oxi-

**Table I** Changes in Weight Average Molecular Weight ( $\bar{M}_w$ ), Number Average Molecular Weight ( $\bar{M}_n$ ), and Polydispersity ( $\bar{M}_w/\bar{M}_n$ ) for Unaged Samples and Samples Aged at 60 and 100°C for 14 Days

Sample	$\bar{M}_n$ (g/mol)	$\bar{M}_w$ (g/mol)	$\bar{M}_w/\bar{M}_n$
LDPE unaged	10,900	79,000	7.3
LDPE aged at 60°C	10,900	75,600	7.0
LDPE aged at 100°C	1100	5200	4.7
LDPE-SBR unaged	11,500	79,400	6.9
LDPE-SBR aged at 60°C	2300	9900	4.3
LDPE-SBR aged at 100°C	500	1400	2.8
LDPE-NR unaged	9900	77,300	7.8
LDPE-NR aged at 60°C	1600	9000	5.6
LDPE-NR aged at 100°C	470	1255	2.7

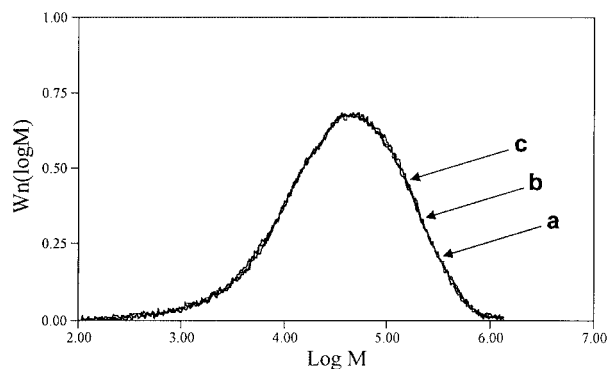


**Figure 2** Molecular weight distributions of samples before thermal treatment (unaged material): (a) LDPE, (b) LDPE-SBR, (c) LDPE-NR.

dation of the polyethylene. There are larger amounts of oxidizable sites (unsaturation) in the domains containing NR than in those containing SBR, and this in turn increases the possibility of hydroperoxide formation and thereby increases the rate of thermo-oxidation of LDPE.

Table I shows a summary of the observed weight average molecular weight ( $\overline{M}_w$ ), number average molecular weight ( $\overline{M}_n$ ), and polydispersity for unaged samples, and for samples aged at 60 and 100°C for 14 days. Figures 2–4 show overlay plots of the molecular weight distributions for these samples. Figure 2 demonstrates the similarity in the molecular weight distributions of the three unaged materials. For both LDPE-SBR-60°C and LDPE-NR-60°C, there appears to be a small decrease in molecular weight and chromatogram peak area because of aging (Fig. 3). There is a much greater decrease in the molecular weight and chromatogram peak area in the case

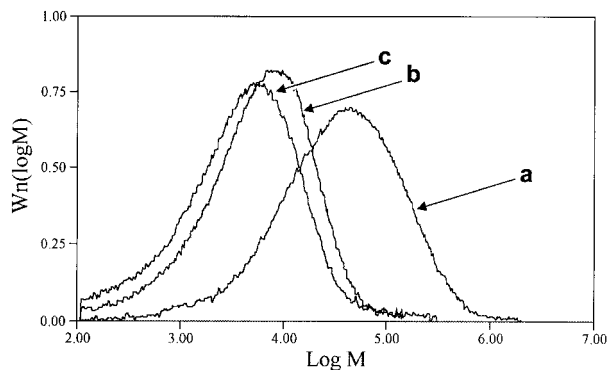


**Figure 3** Molecular weight distributions of samples after treatment at 60°C for a period of 14 days: (a) LDPE, (b) LDPE-SBR, (c) LDPE-NR.

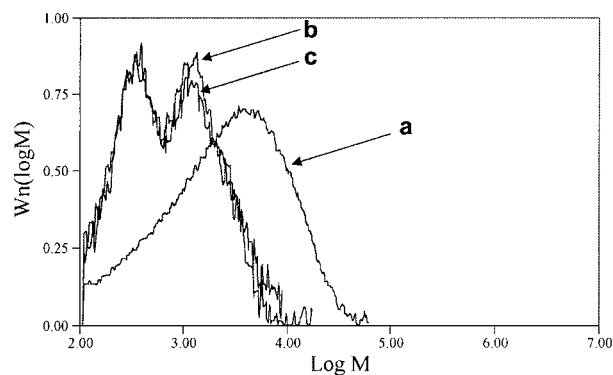


**Figure 4** Molecular weight distributions of samples after treatment at 100°C for a period of 14 days: (a) LDPE, (b) LDPE-SBR, (c) LDPE-NR.

of the samples aged at 100°C (Fig. 4). In the LDPE-100°C samples, the decrease in molecular weight and the chromatogram peak area is much less than in the LDPE-SBR-100°C and LDPE-NR-100°C samples. The decrease in chromatogram peak area indicates that the polymer has become less soluble and that there has probably been some crosslinking to give an insoluble gel. Crosslinking will statistically involve the longer polymer chains and the observed decrease in molecular weight could be attributed to chain scission or to the removal of higher molecular weight material as gel or a combination of both of these reactions. The results indicate that LDPE-SBR and LDPE-NR have a similar effect on the degradation of LDPE, but the rate of degradation appears to be greater for the LDPE-NR than for the LDPE-SBR.

Table II shows the mass crystallinity and melting temperature for the unaged materials (LDPE, LDPE-SBR, and LDPE-NR) and for the same materials aged at 60 and 100°C. All the materials show an increase in crystallinity after aging at 60°C (first heating run). The increase in crystallinity is greater for LDPE-NR (approximately 8%) than for LDPE-SBR (approximately 4%) and LDPE (approximately 2%). The increase in crystallinity is due to both annealing and oxidation followed by the scission of constrained chains in the amorphous region. The chain scission leads to relaxation of local stresses and this allows the released chains to crystallize.<sup>20,21</sup> Secondary crystallization of smaller molecules that have been formed by chain scission because of aging may also contribute to the crystallinity increase. The mass crystallinity of LDPE-SBR and LDPE-NR samples after aging at 100°C showed a decrease.

**Table II** Changes in Mass Crystallinity and Melting Temperature for Unaged Samples and Samples Aged at 60 and 100°C, Respectively

Sample	First Heating Run		Second Heating Run	
	Crystallinity (%)	$T_m$	Crystallinity (%)	$T_m$
LDPE unaged	32	110	35	110
LDPE aged at 60°C	35	110	36	109
LDPE aged at 100°C	33	115	30	113
LDPE-SBR unaged	33	109	35	109
LDPE-SBR aged at 60°C	37	110	36	110
LDPE-SBR aged at 100°C	27	123	23	119
LDPE-NR unaged	32	109	36	109
LDPE-NR aged at 60°C	41	110	35	111
LDPE-NR aged at 100°C	26	124	23	119

This decrease was probably a result of the disruption of the crystalline order by oxidation. In addition, the formation of crosslinks, chain branches, and oxidation products may also prohibit the crystallization of the material on subsequent cooling from 100°C to room temperature and this contributes to this decrease.<sup>22,23</sup>

Figure 5 shows the DSC melting curves of unaged samples and samples aged at 60 and 100°C for 14 days. The melting behavior of the unaged samples is almost the same for all the materials. Likewise, the samples aged at 60 and 100°C showed the same melting behavior at the respective temperatures.

The melting peaks of all the samples became smaller and sharper after aging at 100°C and the melting temperature was shifted to a higher temperature. The greatest increase in the melting temperature was observed for LDPE-NR. These changes in the melting peaks and melting temperatures are probably attributable to the formation of more uniform and perfect crystals during the degradation, and these melt at higher temperature.

TGA analysis was used to provide information regarding mass loss of the samples as a function of time and the derivative of the mass loss as a function of time.

Figure 6(a,b) shows the mass loss and the derivatized of the mass loss of LDPE, LDPE-SBR, and LDPE-NR at 100°C during a period of 14 days. As shown in Figure 6(a), a mass increase was initially observed for LDPE-SBR and LDPE-NR samples and no oxidation induction time can be determined. The mass passes through a maximum, and thereafter a continuous decrease in

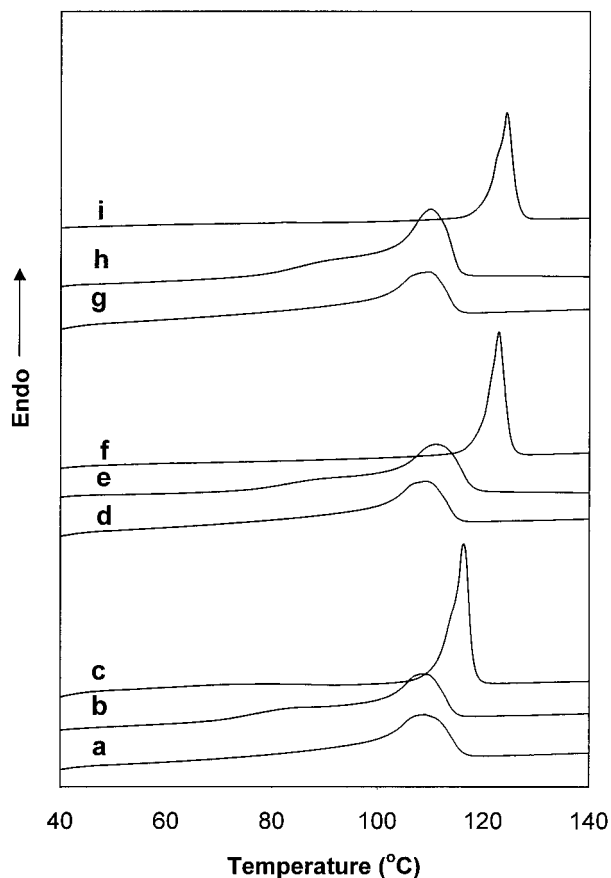
mass is detected. The maximum mass is reached more rapidly for LDPE-NR (after about 2.5 days) than for LDPE-SBR (after about 4.5 days) [Fig. 6(a)]. The decrease in mass also occurs more rapidly in LDPE-NR than in LDPE-SBR. The initial increase in mass is a result of oxygen uptake. The reaction of oxygen with radicals leads to the formation of hydroperoxides that are unstable toward heat and decompose to free radicals. Transition metal ions catalyze the decomposition of hydroperoxides to the free radicals, and this results in chain scission and the formation of oxidation products such as carbonyl compounds.<sup>9,10,24,25</sup> The release of volatile compounds leads to a mass decrease.

These results show that thermo-oxidation is apparently faster in LDPE-NR than in LDPE-SBR. Because the amount of manganese stearate is the same in both LDPE-SBR and LDPE-NR samples, the accelerating effect must be attributed to the rubber phase in the pro-oxidant formulation. The NR phase in the LDPE-NR is more susceptible to oxidation than the SBR phase in the LDPE-SBR, because of the presence of a larger amount of oxidizable sites in the former sample than in the latter.

LDPE showed an induction time of approximately 1.5 days before the mass of the sample started to increase. This mass increase continued slowly during the test period and no significant decrease in mass was observed.

The DTG curves [Fig. 6(b)] also clearly show the differences between the maxima in the degradation rates of LDPE-NR and LDPE-SBR.

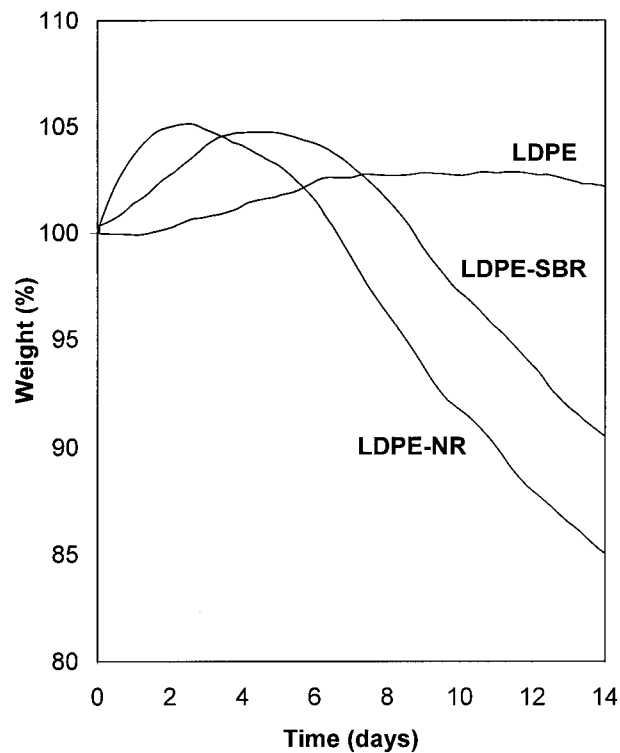
Oxidation of polyethylene leads to the accumulation of carbonyl-containing products.<sup>26,27</sup> Fig-



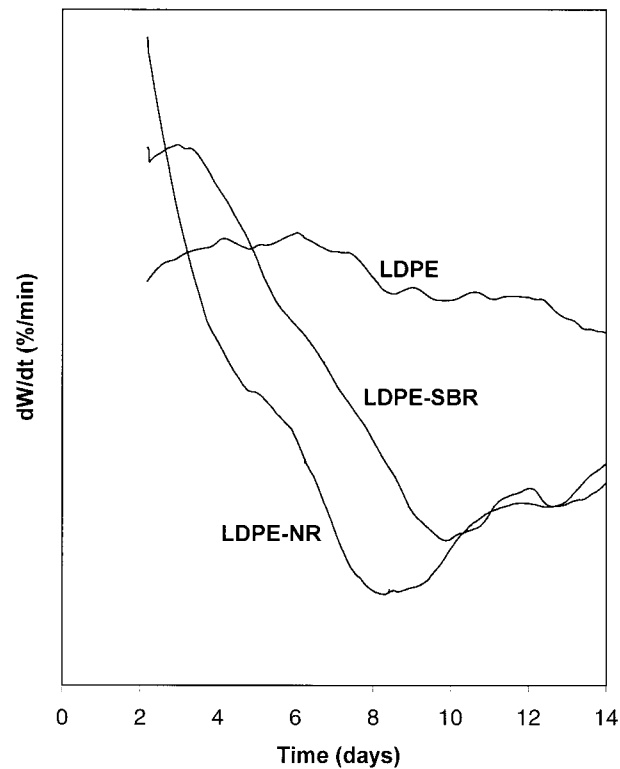
**Figure 5** DSC thermograms of (a) unaged LDPE, (b) LDPE aged at 60°C for a period of 14 days, (c) LDPE aged at 100°C for a period of 14 days, (d) unaged LDPE-SBR, (e) LDPE-SBR aged at 60°C for a period of 14 days, (f) LDPE-SBR aged at 100°C for a period of 14 days, (g) unaged LDPE-NR, (h) LDPE-NR aged at 60°C for a period of 14 days, (i) LDPE-NR aged at 100°C for a period of 14 days. (First heating run.)

Figure 7 shows the FTIR spectrum of unaged samples and of samples aged at 60 and 100°C, for 14 days. The carbonyl region ( $1850\text{--}1550\text{ cm}^{-1}$ ) showed several overlapping absorption bands. The absorptions at  $1712$ ,  $1723$ ,  $1740$ , and  $1780\text{ cm}^{-1}$  have been assigned to carboxylic acid, ketone, ester, and  $\gamma$ -lactone, respectively.<sup>28,29</sup>

After treatment at 100°C, both LDPE-NR and LDPE-SBR show a strong absorption band at  $1160\text{ cm}^{-1}$  that is attributed to the carbon-oxygen single bond. According to the FTIR data, the formation of carbonyl compounds was faster in the LDPE-NR and LDPE-SBR than in the LDPE, but the development in both the carbonyl and carbon-oxygen single-bond regions was very similar for both the LDPE-NR and the LDPE-SBR.



(a)



(b)

**Figure 6** (a) TGA, (b) DTG curves of LDPE, LDPE-SBR, and LDPE-NR in  $O_2$  atmosphere at 100°C for 14 days.

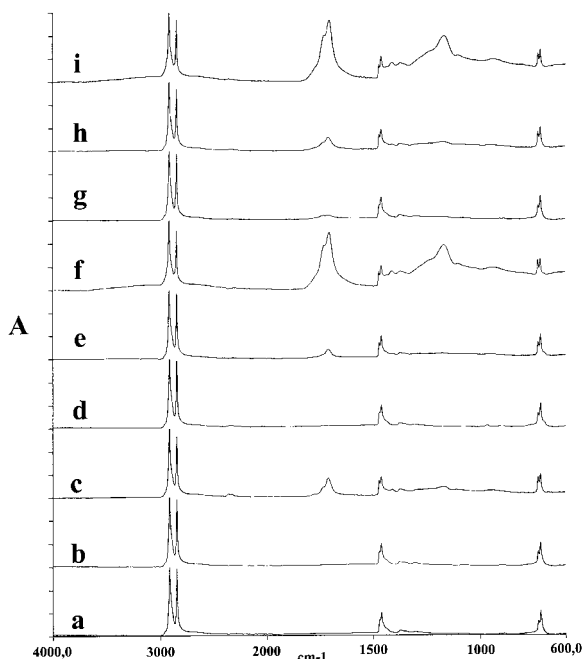


**Figure 7** FTIR spectra of (a) unaged LDPE, (b) LDPE aged at 60°C for a period of 14 days, (c) LDPE aged at 100°C for a period of 14 days, (d) unaged LDPE-SBR, (e) LDPE-SBR aged at 60°C for a period of 14 days, (f) LDPE-SBR aged at 100°C for a period of 14 days, (g) unaged LDPE-NR, (h) LDPE-NR aged at 60°C for a period of 14 days, (i) LDPE-NR aged at 100°C for a period of 14 days.

## CONCLUSIONS

Extensive investigations using CL, SEC, DSC, TGA, and FTIR have enabled the following conclusions to be drawn:

1. CL measurements show clearly that the rate of oxidation is faster in LDPE-NR than in LDPE-SBR. Furthermore, the final damaging effect of the pro-oxidant in LDPE-NR is higher than that of the pro-oxidant in LDPE-SBR.
2. SEC results demonstrate that blending LDPE with SBR or NR has a similar effect on degradation, but the degradation appears to be faster in the case of the LDPE-NR than in the LDPE-SBR.
3. Based on DSC data, changes in mass crystallinity and melting temperature are higher for LDPE-NR than for LDPE-SBR. However, the melting behavior of both samples is almost the same after aging at 60 or 100°C.
4. TGA and DTG results clearly show that thermo-oxidation is faster and more effective in LDPE-NR than in LDPE-SBR, which reconfirmed the CL results.
5. All of these techniques were found to be useful in this study, but CL and TGA were the most effective techniques for establishing the differences between the various pro-oxidant systems. The use of only these two techniques is an excellent way of showing the differences between various pro-oxidant systems.

We thank Petter Ericsson and Dr. Karin Jacobson for help with the CL instrument and for valuable discussions.

## REFERENCES

1. Albertsson, A. C.; Rånby, B.; In Proceedings of the 3rd International Biodegradation Symposium; Kingston, RI; Sharpley, J. M.; Kaplan, A. M., Eds.; Applied Sciences Publishers: London, 1975, p. 743.
2. Albertsson, A. C.; Karlsson, S. *J Appl Polym Sci* 1988, 35, 1289.
3. Amin, M. U.; Scott, G. *Eur Polym J* 1974, 10, 1019.
4. Al-Malaika, S.; Chakraborty, K. B.; Scott, G. In *Developments in Polymer Stabilization-6*; Scott, G., Ed.; Applied Science Publishers: London, 1983, 73.
5. Griffin, G. J. L. U. S. Pat. 4,016,117, 1977.
6. Griffin, G. J. L. U. S. Pat. 4,021,388, 1977.
7. Griffin, G. J. L. U. S. Pat. 4,218,350, 1980.
8. Griffin, G. J. L. U. S. Pat. 4,983,651, 1991.
9. Khabbaz, F.; Albertsson, A. C.; Karlsson, S. *Polym Degrad Stab* 1998, 61, 329.
10. Khabbaz, F.; Albertsson, A. C.; Karlsson, S. *Polym Degrad Stab* 1999, 63, 127.
11. Hakkarainen, M.; Albertsson, A. C.; Karlsson, S. *J Appl Polym Sci* 1997, 66, 959.
12. Albertsson, A. C.; Barenstedt, C.; Karlsson, S. *Polym Degrad Stab* 1992, 37, 163.
13. Scott, G. In *Atmospheric Oxidation and Antioxidants*; Scott, G., Ed.; Elsevier Publishing: Amsterdam, 1965; Chapter 3.
14. Wunderlich, B. *Macromolecular Physics*; Academic Press: New York, 1973; Chapter 8.
15. Gorge, G. A.; In *Luminescence Techniques in Solid State Polymer Research*; Zlatkevich, L., Ed.; Marcel Dekker: New York, 1989; Chapter 3.
16. Billingham, N. C.; Then, E. T. H.; Gijnsman, P. J. *Polym Degrad Stab* 1991, 34, 263.
17. Matisova-Rychla, L.; Fodor, Zs.; Rychly, J.; Iring, M. *Polym Degrad Stab* 1980–1981, 3, 371.
18. Kron, A.; Stenberg, B.; Reitberger, T.; Billingham, N. C. *Polym Degrad Stab* 1996, 53, 119.

19. Albertsson, A. C.; Barenstedt, C.; Karlsson, S. *J Appl Polym Sci* 1994, 51, 1097.
20. Winslow, F. H. *Pure Appl Chem* 1977, 49, 495.
21. Billingham, N. C.; Prentice, P.; Walker, T. J. *J Polym Sci Polym Symp* 1976, 57, 287.
22. Rosen, P.; Reitberger, T.; Gubanski, S. M.; Gedde, U. W. *IEEE Trans Die Elect Insul* 1999, 6, 191.
23. Khraishi, N.; Al-Rebaidi, A. *Polym Degrad Stab* 1991, 32, 105.
24. Albertsson, A. C.; Karlsson, S.; *Makromol Chem Macromol Symp* 1991, 48/49, 395.
25. Barabas, K.; Iring, M.; Kelen, T.; Tudos, F. *J Polym Sci Polym Symp* 1976, 57, 65.
26. Lacoste, J.; Carlsson, D. J.; Falicki, S.; Wiles, D. M. *Polym Degrad Stab* 1991, 34, 309.
27. Gugumus, F. *Polym Degrad Stab* 1996, 52, 131.
28. Luongo, J. P. *J Polym Sci* 1990, 42, 139.
29. Singh, R. P.; Mani, R.; Sivaram, S.; Lacoste, J.; Vaillant, D. *J Appl Polym Sci* 1993, 50 871.